

## Two-color fluorescent L-amino acid mimic of tryptophan for probing peptide-nucleic acid complexes

Aleksandr V Strizhak, Viktoriia Y Postupalenko, Volodymyr V Shvadchak, Nelly Morellet, Eric Guittet, Vasyl G Pivovarenko, Andrey S Klymchenko, and Yves Mély

*Bioconjugate Chem.*, **Just Accepted Manuscript** • Publication Date (Web): 16 Nov 2012

Downloaded from <http://pubs.acs.org> on November 19, 2012

### Just Accepted

"Just Accepted" manuscripts have been peer-reviewed and accepted for publication. They are posted online prior to technical editing, formatting for publication and author proofing. The American Chemical Society provides "Just Accepted" as a free service to the research community to expedite the dissemination of scientific material as soon as possible after acceptance. "Just Accepted" manuscripts appear in full in PDF format accompanied by an HTML abstract. "Just Accepted" manuscripts have been fully peer reviewed, but should not be considered the official version of record. They are accessible to all readers and citable by the Digital Object Identifier (DOI®). "Just Accepted" is an optional service offered to authors. Therefore, the "Just Accepted" Web site may not include all articles that will be published in the journal. After a manuscript is technically edited and formatted, it will be removed from the "Just Accepted" Web site and published as an ASAP article. Note that technical editing may introduce minor changes to the manuscript text and/or graphics which could affect content, and all legal disclaimers and ethical guidelines that apply to the journal pertain. ACS cannot be held responsible for errors or consequences arising from the use of information contained in these "Just Accepted" manuscripts.



**ACS Publications**  
High quality. High impact.

Bioconjugate Chemistry is published by the American Chemical Society, 1155 Sixteenth Street N.W., Washington, DC 20036  
Published by American Chemical Society. Copyright © American Chemical Society. However, no copyright claim is made to original U.S. Government works, or works produced by employees of any Commonwealth realm Crown government in the course of their duties.

# Two-color fluorescent L-amino acid mimic of tryptophan for probing peptide-nucleic acid complexes

*Aleksandr V. Strizhak,<sup>‡,§,†</sup> Viktoriia Y. Postupalenko,<sup>‡,§</sup> Volodymyr V. Shvadchak,<sup>§,¶</sup> Nelly Morellet,<sup>⊥</sup> Eric Guittet,<sup>⊥</sup> Vasyl G. Pivovarenko,<sup>†§</sup> Andrey S. Klymchenko,<sup>\*,§</sup> Yves Mély,<sup>\*,§</sup>*

<sup>§</sup>Laboratoire de Biophotonique et Pharmacologie, UMR 7213 CNRS, Université de Strasbourg, Faculté de Pharmacie, 67401 Illkirch, France

<sup>†</sup>Department of Chemistry, National Taras Shevchenko University of Kyiv, 01601 Kyiv, Ukraine

<sup>⊥</sup>CNRS UPR 2301, Chimie et biochimie structurales, Institut de Chimie des Substances Naturelles, Centre de recherche de Gif-sur-Yvette, 91190 Gif-sur-Yvette, France

**RECEIVED DATE (to be automatically inserted after your manuscript is accepted if required according to the journal that you are submitting your paper to)**

<sup>‡</sup> AVS and VYP equally contributed to this work

\*CORRESPONDING AUTHOR FOOTNOTE: [andrey.klymchenko@unistra.fr](mailto:andrey.klymchenko@unistra.fr) ; [yves.mely@unistra.fr](mailto:yves.mely@unistra.fr);  
Tel: +33 368 854255, +33 368 854263. Fax: +33 368 854313.

RUNNING TITLE: fluorescent L-amino acid

## ABSTRACT

Non-natural amino acids are important tools for site-selective probing of peptide properties and interactions. Here, for the first time a fluorescent L-amino acid, exhibiting excited-state intramolecular proton transfer (ESIPT) and hydration-sensitive dual emission, was synthesized. It is an analogue of L-tryptophan bearing a slightly larger 2-(2-furyl)-3-hydroxychromone aromatic moiety instead of indole. This new amino acid was incorporated through solid phase synthesis into NC(11-55), the zinc finger domain of the HIV-1 nucleocapsid protein, that exhibits potent nucleic acid chaperone properties. It was substituted for the Trp37 and Ala30 residues, located in the distal finger motif and the linker between the fingers of NC(11-55), respectively. Though the highly conserved Trp37 residue plays a key role in NC(11-55) structure and activity, its substitution for the new fluorescent analogue preserved the folding, the nucleic acid binding and chaperone activity of the peptide, indicating that the new amino acid can conservatively substitute Trp residues. In the presence of oligonucleotides, the Trp37-substituted peptide, but not the Ala30 variant, showed strong changes of their dual emission corresponding to local dehydration. The results are in line with NMR data, suggesting that the fluorescent amino acid interacts similarly to Trp37 with the nucleobases and is thus screened from water. Due to the exceptional sensitivity of its ESIPT fluorophore to hydration in highly polar environment, the new amino acid appears as a promising tool for substituting Trp residues and site-selectively investigating peptide-nucleic acid complexes.

## Introduction

Non-natural amino acids are important tools to investigate peptides and proteins, since they can be incorporated at any position, and thus, serve as local probes for site-selective monitoring of protein properties and functions. Probably, the most popular ones are those bearing fluorine (1-4) and dyes (5-7) used with NMR and fluorescence techniques, respectively. Fluorescent amino acids are particularly attractive, due to the ultimate sensitivity of fluorescence-based methods. Since the natural fluorescent amino acid tryptophan suffers from poor fluorescence properties, continuous efforts have been done to design amino acids with improved fluorophores (5-7). Of special interest in this respect are environment-sensitive (or solvatochromic) fluorophores, which change their emission properties in response to changes in their environment (7, 8). Biomolecular interactions commonly decrease the polarity at the labeling site due to screening from water and thus, can be readily monitored by environment-sensitive fluorescent amino acids (7). For instance, a Prodan-based amino acid was used for monitoring the interaction of S-peptide with ribonuclease S (9) and  $\delta$ -opioid receptor with antagonists (10) and to estimate the local dielectric constant of the B1 domain of the staphylococcal protein G (5). Moreover, an amino acid based on 4-dimethylaminophthalimide (4-DMAP) fluorophore was applied to sense binding of labeled octapeptides to the 14-3-3bp protein (11). Finally, improved analogues of 4-DMAP, such as 6-dimethylaminonaphthalimide, were recently applied to investigate the SH2 phosphotyrosine binding domains (12), major histocompatibility complexes (MHC) at the cell surface (7) and peptide-calmodulin interactions (13). Despite the importance of environment-sensitive fluorescent amino acids in biomolecular research, their examples are limited.

Moreover, most examples are focused on protein-protein interactions (7), while applications of fluorescent amino acids for sensing peptide-oligonucleotide (ODNs) interactions have been poorly explored (Figure 1A). To address this problem, we selected 3-hydroxychromone (3HC) fluorophores which undergo excited-state intramolecular proton transfer (ESIPT) (14), resulting in the emission of both a normal (N\*) excited state and an ESIPT product tautomer (T\*) (Figure 1B). The dual emission of 3HC dyes is highly sensitive to polarity and H-bonding interactions (8, 15-23). The 2-(2-furyl)-3-hydroxychromone (FHC) label is particularly interesting due to the high sensitivity of its dual emission to polar environments (15, 17, 24, 25). Being attached to the N-terminus of peptides and oligocations, it shows strong changes in its dual emission upon interaction with ODNs (26, 27), and allows quantification of water content in its surrounding (28). This prompted us to develop an L-amino acid based on the FHC fluorophore.

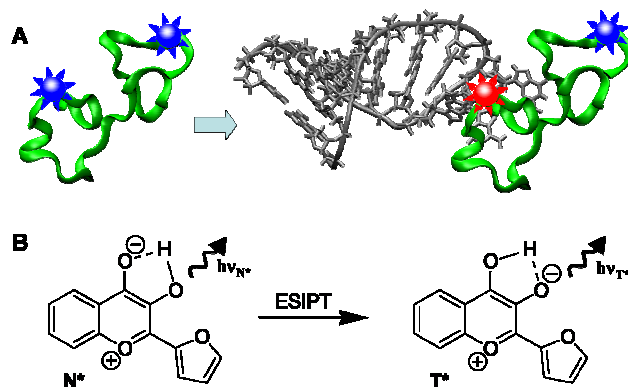


**Figure 1.** Monitoring of peptide/oligonucleotide interaction using solvatochromic fluorescent amino acid. (A) Principle: the interaction of the labeled peptide (in green) with oligonucleotides changes the fluorescence intensity and color of the label. (B) ESIP T reaction in 2-(2-furyl)-3-hydroxychromone dye.

As a target protein for labeling, we selected the nucleocapsid protein (NC) of the Human Immunodeficiency Virus, type 1 (HIV-1), which plays a crucial role in the viral life cycle (29, 30). NC is a small (55 amino acids) basic protein, characterized by two rigid zinc fingers connected by a flexible basic linker and flanked by poorly folded N- and C-terminal basic domains (31, 32). NC binds both specifically (33-38) and non-specifically (35, 39-41), to a large range of nucleic acid sequences. Specific binding is mainly mediated through the folded finger motifs, with a key role being played by the hydrophobic residues forming a hydrophobic platform at the top of the folded fingers (34, 36, 38). This hydrophobic plateau plays also a key role in the nucleic acid chaperone properties of NC, which enable to direct the structural rearrangement of ODNs into their most stable conformation and promote the annealing of complementary ODN sequences through specific pathways (42-44). Within this hydrophobic plateau, the Trp37 residue plays a particularly important role, since its substitution by a non-aromatic residue leads to a dramatic decrease in ODN affinity (35, 40, 45), a complete loss in the highly specific ODN destabilization component of the NC chaperone properties (40, 42) as well as a complete loss of HIV-1 infectivity (46). In the present work, we synthesized an L-amino acid analogue based on 2-(2-furyl)-3-hydroxychromone dye through an original route from L-tyrosine. It was then incorporated at two different positions of the NC(11-55), inside and outside of its fingers, which allowed us to site-selectively investigate its interaction with ODNs. Remarkably, substitution of Trp residue for the new amino acid marginally alters the folding as well as the nucleic acid binding and chaperone activity of the peptide, indicating that this new amino acid could be used as a Trp mimic. The ODNs selected for binding (Figure S1, Supporting Information) to the labeled peptides were SL2 and

SL3, two stem-loops of the HIV-1 RNA encapsidation sequence (33, 35, 38) and  $\Delta P(-)$ PBS, the cDNA copy of the primer binding site, deleted of its 5' overhang (36). These three ODNs bind NC with high affinity and 1:1 stoichiometry, and their structures in complex with NC are known (34, 36, 38). The results showed that this amino acid allows probing protein sites responsible for DNA binding.

## Materials and methods

All the solvents and chemicals were purchased from Sigma-Aldrich Chemical Company. For absorption and fluorescence studies, the solvents were of spectroscopic grade.  $\Delta P(-)$ PBS DNA, SL2 and SL3 RNAs were synthesized and HPLC-purified by IBA GmbH (Germany). Concentrations of the ODNs were calculated from their absorbance using the molar extinction coefficients at 260 nm provided by the supplier.

NMR spectra were recorded on a 400 MHz and 500 MHz BrukerAvance III, BBFO+ at room temperature. Mass spectra were obtained on a Bruker HCT Ultra and Agilent Technologies Accurate-Mass Q-TOF LC/MS 6520 mass spectrometers.

**Synthesis of Fmoc-3HCaa.** The synthesis of the compounds 1 and 2 (Scheme S1) was performed as described previously (47, 48).

*N*-(*tert*-butoxycarbonyl)-3-[(2*E*)-3-(2-furyl)prop-2-enoyl]-*L*-tyrosine (**3**). 6.425 g (19.89 mmol) of 3-acetyl-*N*-(*tert*-butoxycarbonyl)-*L*-tyrosine **2** were dissolved in 48 ml of ethanol upon stirring under Ar atmosphere. To the reaction mixture, 48 ml of degassed 25% solution of sodium hydroxide was added upon cooling in cold water bath. Then, 2.409 g of furfural (25.09 mmol, 1.26 eq.) were added and the mixture was stirred for 12 h at RT under Ar. Additional 0.5 g of furfural was added and the mixture was stirred overnight. The reaction mixture was acidified with HCl and diluted twice with water. The formed precipitate was filtered and washed with diluted ethanol and water, dried and used in the next step without further purification. Yield 7.62 g (95%) of chalcone **3** as a yellow powder. <sup>1</sup>H-NMR (500 MHz, MeOD)  $\delta$  1.33 (s, 9H), 2.87-2.92 (dd,  $J = 13.9$  Hz,  $J = 8.85$  Hz, 1H), 3.16-3.19 (dd,  $J = 13.9$  Hz,  $J = 4.43$  Hz, 1H), 4.31-4.34 (dd,  $J = 8.85$  Hz,  $J = 4.43$  Hz, 1H), 6.61-6.62 (dd,  $J = 3.16$  Hz,  $J = 1.89$  Hz, 1H), 6.87-6.89 (d,  $J = 8.21$  Hz, 1H), 6.94 (d,  $J = 3.8$  Hz, 1H), 7.39-7.41 (dd,  $J = 8.22$  Hz,  $J = 1.9$  Hz, 1H), 7.64-7.71 (dd,  $J = 15.16$  Hz,  $J = 4.42$  Hz, 2H), 7.71 (d,  $J = 1.9$  Hz, 1H), 7.86-7.87 (d,  $J = 1.9$  Hz, 1H). <sup>13</sup>C-NMR (500 MHz, MeOD)  $\delta$  28.66, 38.11, 55.49, 80.47, 114.01, 118.33, 118.84, 119.02, 120.97, 129.45, 131.65, 132.31, 138.58, 147.17, 152.98, 157.68, 163.09, 175.69, 194.74 (two carbon signals are absent due to incidental equivalence). HRMS (EI)  $m/z$  calcd for C<sub>21</sub>H<sub>23</sub>NO<sub>7</sub> 401.14745, found: 401.147.

*N*-(*tert*-butoxycarbonyl)-3-[2-(2-furyl)-3-hydroxy-4-oxo-4*H*-chromen-6-yl]-*L*-alanine (**4**). 7.62 g (19 mmol) of chalcone **3** was dissolved in 75 ml of ethanol, cooled in ice bath. Then, 75 ml of 1M solution of sodium hydroxide was added with stirring. Next, 4.73 ml (41.8 mmol) of 30% hydrogen peroxide was added and the mixture was stirred in ice bath for 4 h. The reaction was monitored by TLC (silica, EtOAc/MeOH 9:1). After completing the reaction, the mixture was acidified and the formed precipitate was filtered. Yield of the crude 3-hydroxychromone **4** was 3.56 g (45%). It was purified to about 95% purity by crystallization several times from toluene and then from acetonitrile. Final yield ~ 1.5 g (20%) of yellow crystals. <sup>1</sup>H-NMR (500 MHz, MeOD) δ 1.33 (s, 9H), 2.98-3.03 (dd, *J* = 13.9 Hz, *J* = 9.48 Hz, 1H), 3.26-3.30 (m, *J* = 5.05 Hz, 1H), 4.36-4.39 (dd, *J* = 9.48 Hz, *J* = 5.05 Hz, 1H), 6.67 (m, 1H), 7.33 (d, *J* = 3.16 Hz, 1H), 7.51-7.53 (d, *J* = 8.85 Hz, 1H), 7.60-7.62 (d, *J* = 8.85 Hz, 1H), 7.78 (s, 1H), 7.97 (d, *J* = 1.27 Hz, 1H). <sup>13</sup>C-NMR (500 MHz, MeOD) δ 28.6, 38.27, 56.26, 80.52, 113.58, 116.91, 119.29, 122.83, 126.26, 135.77, 135.97, 138.44, 141.29, 145.86, 146.08, 155.09, 157.77, 173.81, 175.11 (two carbon signals are absent due to incidental equivalence). HRMS (EI) *m/z* calcd for C<sub>21</sub>H<sub>21</sub>NO<sub>8</sub> 415.12672, found: 415.12659.

3-[2-(2-furyl)-3-hydroxy-4-oxo-4*H*-chromen-6-yl]-*L*-alanine hydrochloride (**5**). 944 mg of 3-hydroxychromone **4** was dissolved in 10 ml of dioxane. Then, 10 ml of conc. HCl was added to the reaction mixture in cold water bath. After 5-10 min, the bath was removed and the mixture was stirred for 2-3 h. The reaction mixture was concentrated under reduced pressure to give the desired product **5** as a dark yellow powder, yield 0.769 g (96%). <sup>1</sup>H-NMR (500 MHz, MeOD) δ 3.28-3.34 (dd, *J* = 14.56 Hz, *J* = 7.78 Hz, 1H), 3.42-3.48 (dd, *J* = 14.56 Hz, *J* = 5.77 Hz, 1H), 4.34-4.37 (dd, *J* = 7.53 Hz, *J* = 5.77 Hz, 1H), 6.7-6.72 (dd, *J* = 3.52 Hz, *J* = 1.76 Hz, 1H), 7.37-7.38 (d, *J* = 3.51 Hz, 1H), 7.63-7.65 (d, *J* = 8.79 Hz, 1H), 7.68-7.71 (dd, *J* = 8.79 Hz, *J* = 2.26 Hz, 1H), 7.81-7.82 (d, *J* = 1.00 Hz, 1H), 8.05-8.06 (d, *J* = 1.76 Hz, 1H). <sup>13</sup>C-NMR (500 MHz, MeOD) δ 36.74, 54.95, 113.70, 117.23, 120.29, 123.34, 126.81, 132.56, 135.79, 138.64, 141.67, 145.83, 146.33, 155.71, 171.00, 173.74. HRMS (EI) *m/z* calcd for C<sub>16</sub>H<sub>13</sub>NO<sub>6</sub> 315.07429, found: 315.07419.

*N*-[(9*H*-fluoren-9-ylmethoxy)carbonyl]-3-[2-(2-furyl)-3-hydroxy-4-oxo-4*H*-chromen-6-yl]-*L*-alanine (**6**). 614 mg (1.744 mmol) of amino acid hydrochloride **5** was dissolved in a solution of 500 mg (5.95 mmol) of sodium bicarbonate in 10 mL of water. Then, 30 mL of acetonitrile and 588 mg (1 eq.) of FmocOSu were added and the mixture was stirred for 24 h. The reaction mixture was filtered and the precipitate was dissolved in hot water (about 100 mL per 1 g) with further acidification with HCl. Yield 900 mg (96%) of yellow powder. <sup>1</sup>H-NMR (500 MHz, DMSO-*d*<sub>6</sub>) δ 3.00-3.05 (m, 1H), 3.22-3.26 (dd, *J* = 14.04 Hz, *J* = 4.27 Hz, 1H), 4.12-4.19 (m, 3H), 4.26-4.30 (m, 1H), 6.77-6.78 (dd, *J* = 3.05 Hz, *J* = 1.83 Hz, 1H), 7.21-7.25 (m, 2H), 7.27-7.28 (d, *J* = 3.05 Hz, 1H), 7.34-7.37 (t, *J* = 7.32 Hz, 2H), 7.57-

7.58 (d,  $J = 7.32$  Hz, 2H), 7.59-7.61 (d,  $J = 8.55$  Hz, 1H), 7.68-7.70 (d,  $J = 8.55$  Hz, 1H), 7.75-7.76 (d,  $J = 8.55$  Hz, 1H), 7.82-7.83 (d,  $J = 7.32$  Hz, 2H), 8.01 (s, 1H), 8.04 (s, 1H), 9.88 (s, 1H), 12.76 (br s, 1H).  $^{13}\text{C}$ -NMR (500 MHz, DMSO- $d_6$ )  $\delta$  35.80, 46.54, 55.39, 65.64, 112.82, 115.27, 118.03, 120.04, 121.56, 124.95, 125.11, 125.18, 126.98, 127.55, 134.68, 137.20, 139.19, 140.63, 143.67, 144.09, 145.17, 152.96, 156.01, 171.78, 173.07 (six carbon signals are absent due to incidental equivalence). HRMS (EI)  $m/z$  calcd for  $\text{C}_{31}\text{H}_{23}\text{NO}_8$  537.14237, found: 537.14187.

**Proof of optical purity.** To test the enantiomeric purity of the obtained chromone-amino acid derivative, we prepared the dibenzyl ether-ester of the amino acid, which was acylated by two enantiomers of Mosher's acid chloride to give compounds **9** and **10** (Scheme S1). The NMR spectra of the diastereomeric Mosher amides were then compared. No signal of the second diastereomer was found in each spectrum.

*Benzyl 3-[3-(benzyloxy)-2-(2-furyl)-4-oxo-4H-chromen-6-yl]-N-[(2S)-3,3,3-trifluoro-2-methoxy-2-phenylpropanoyl]-L-alaninate (9).*  $^1\text{H}$ -NMR (400 MHz,  $\text{CDCl}_3$ )  $\delta$  3.14-3.19 (dd,  $J = 14.24$  Hz,  $J = 7.12$  Hz, 1H), 3.20 (s, 3H), 3.24-3.29 (dd,  $J = 14.24$  Hz,  $J = 5.60$  Hz, 1H), 4.89-4.94 (dd,  $J = 14.25$  Hz,  $J = 6.62$  Hz, 1H), 5.05-5.08 (d,  $J = 12.21$  Hz, 1H), 5.11-5.14 (d,  $J = 12.21$  Hz, 1H), 5.24 (s, 2H), 6.48-6.49 (dd,  $J = 3.56$  Hz,  $J = 1.52$  Hz, 1H), 7.18-7.44 (m, 17H), 7.59 (d,  $J = 1.01$  Hz, 1H), 7.96 (d,  $J = 1.53$  Hz, 1H).  $^{19}\text{F}$ -NMR (376 MHz,  $\text{CDCl}_3$ )  $\delta$  -69.5 (9), -72.03 (Mosher acid).

*Benzyl 3-[3-(benzyloxy)-2-(2-furyl)-4-oxo-4H-chromen-6-yl]-N-[(2R)-3,3,3-trifluoro-2-methoxy-2-phenylpropanoyl]-L-alaninate (10).*  $^1\text{H}$ -NMR (400 MHz,  $\text{CDCl}_3$ )  $\delta$  3.02-3.07 (dd,  $J = 14.05$  Hz,  $J = 7.53$  Hz, 1H), 3.16-3.21 (dd,  $J = 14.05$  Hz,  $J = 5.52$  Hz, 1H), 3.35 (d,  $J = 1.50$  Hz, 3H), 4.94-5.00 (m,  $J = 5.52$  Hz,  $J = 7.28$  Hz, 1H), 5.07-5.10 (d,  $J = 12.05$  Hz, 1H), 5.14-5.17 (d,  $J = 12.05$  Hz, 1H), 5.20-5.23 (d,  $J = 10.54$  Hz, 1H), 5.23-5.26 (d,  $J = 10.54$  Hz, 1H), 6.49-6.51 (dd,  $J = 3.52$  Hz,  $J = 1.76$  Hz, 1H), 7.01-7.04 (dd,  $J = 8.79$  Hz,  $J = 2.26$  Hz, 1H), 7.05-7.07 (d,  $J = 8.53$  Hz, 1H), 7.17-7.32 (m, 15H), 7.42-7.45 (dd,  $J = 8.29$  Hz,  $J = 1.76$  Hz, 1H), 7.60 (dd,  $J = 1.76$  Hz,  $J = 0.75$  Hz, 1H), 7.84 (d,  $J = 2.26$  Hz, 1H).  $^{19}\text{F}$ -NMR (376 MHz,  $\text{CDCl}_3$ )  $\delta$  -69.41 (10), -72.03 (Mosher acid).

**Peptide synthesis.** The labeled NC(11-55) peptides were synthesized by solid phase peptide synthesis on a 433A synthesizer (ABI, Foster City, CA), according to a previously established protocol (49). The synthesis was performed at a 0.1 mmol scale using the standard fluorenylmethoxycarbonyl (Fmoc)-amino acid-coupling protocol starting from 0.44 mmol/g Wang LL resin. At selected positions of the peptide, the fluorescent amino acid analogue was incorporated by the following procedure. In a flask, 2-4 mole equivalents of the Fmoc-3HCaa were mixed with 4 eq. of HBTU/HOBt coupling solution (in DMF) and 5 eq. of DIEA. This mixture was immediately added to the peptidylresin and shaken at 37°C for 12 h. Then, the resin was washed with 1-methyl-2-pyrrolidone (NMP) and peptide synthesis was

continued on the synthesizer. At the end of the synthesis, the Fmoc-deprotected peptidylresin was isolated and washed with NMP, methanol and dichloromethane.

Cleavage of the peptidylresin and deprotection were performed for 2 h using a 10 mL trifluoroacetic acid (TFA) solution containing water (5%, v/v), phenol (2%, w/v), thioanisole (5%, v/v), triisopropylsilane (2.5%, v/v) and ethanedithiol (2.5%, v/v). The peptide was precipitated using ice-cold diethyl ether and pelleted by centrifugation. The pellet was air-dried for approx. 15 minutes, solubilized with aqueous TFA (0.05 %, v/v) and lyophilized. Purification by HPLC was carried out on a C8 column (uptisphere 300A, 5 $\mu$ m; 250X10, Interchim, France) in water/acetonitrile mixture containing 0.05% TFA with a linear gradient 10 to 35% of acetonitrile for 30 min and monitored at 210 and 360 nm (3HC dye absorption). Obtained peptides were characterized by ESI-MS analysis. NC(11-55)-W37-3HCaa peptide: calculated M = 5245.40, found  $[M+7H]^{7+} = 750.64$  corresponding to M = 5245.38 after deconvolution; NC(11-55)-A30-3HCaa peptide: calculated M = 5360.43, found  $[M+7H]^{7+} = 767.06$  corresponding to M = 5360.37 after deconvolution.

**Preparation of Zn-bound peptides:** Lyophilized labeled peptides were dissolved in water ( $\approx 0.5$  mg in 500  $\mu$ L). Then, about 10  $\mu$ L of this solution was used to determine the peptide concentration using an extinction coefficient of 15,000  $M^{-1}\times cm^{-1}$  at 350 nm. Next, 2.2 molar equivalents of  $ZnSO_4$  were added to the peptide and pH was raised to its final value, by adding buffer. This last step was done only at the end to prevent peptide oxidization. Noticeably, a large excess of  $Zn^{2+}$  ions should be avoided since this ion could affect the 3HC fluorescence.

**NMR structural studies:** The two NC(11-55) conjugates at 0.5 mM concentration in neat water, pH 6.5 at 293 K were studied on an Avance Bruker spectrometer operating at 600.13 MHz equipped with a cryoprobe. A mixing time of 200 ms and a water gate pulse program for water signal suppression in NOESY experiments were used.

**Spectroscopic measurements:** Unless otherwise indicated, the experiments were performed in 10 mM phosphate buffer, pH 6.5, 30 mM NaCl, at 20 $^{\circ}$ C. This low pH was used to prevent deprotonation of the 3-hydroxy group of the 3HC amino acid. Absorption spectra were recorded with a Cary 4000 UV-visible spectrophotometer (Varian). Fluorescence spectra were recorded on FluoroMax3 and FluoroLog spectrofluorimeters (Jobin Yvon) equipped with thermostated cell compartments. Fluorescence spectra were corrected for Raman scattering. Quantum yields were calculated using quinine sulphate in 0.5 M sulphuric acid (quantum yield,  $\phi = 0.577$ ) as a reference (50). Excitation wavelength was 350 nm for 3HCaa.

To determine the affinity of the labeled peptides for the ODNs, fixed amounts of the ODN were titrated with peptides by monitoring the two-band fluorescence of the labeled peptides. For each data

point, the emission of the same concentration of labeled peptide in buffer was subtracted from the signal measured in the presence of the ODN. Affinity constants were determined from direct fitting of the corrected signal to the rewritten Scatchard equation:

$$I = I_0 - \frac{(I_0 - I_t)}{N_t} x \frac{(1 + (P_t + nN_t)K_a) - \sqrt{(1 + (P_t + nN_t)K_a)^2 - 4P_t nN_t K_a^2}}{2K_a} \quad (1)$$

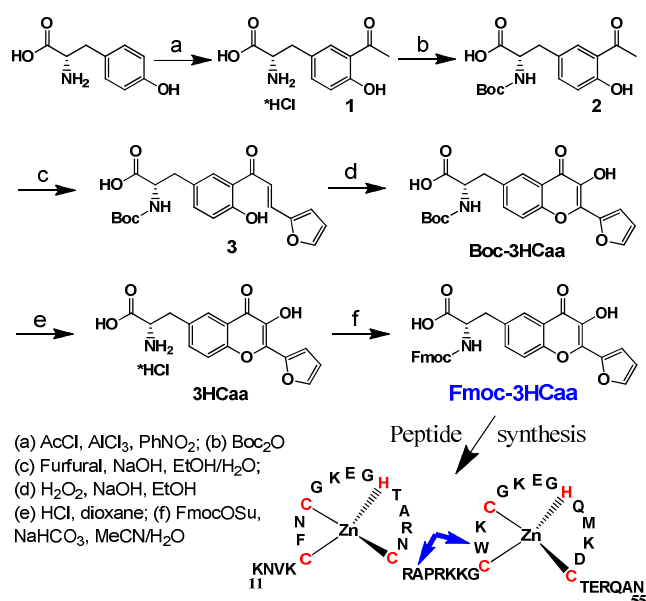
where  $I$  and  $I_t$  are the signal at a given and a saturating peptide concentration, respectively,  $I_0$  is the signal in the absence of peptide,  $N_t$  is the total ODN concentration,  $P_t$  is the total concentration of peptide,  $K_a$  is the apparent affinity constant,  $n$  is the number of binding sites. The parameters were recovered from non-linear fits of equation (1) to experimental datasets using the MicrocalOrigin™ 6.0 software.

**Peptide activity tests.** The ability of the labeled peptides to destabilize the secondary structure of ODNs was tested using cTAR DNA, the complementary sequence of the transactivation response element, involved in the minus strand DNA transfer during reverse transcription. To this end, we used a cTAR sequence labeled at its 3' and 5' ends by 5(6)-carboxytetramethylrhodamine (TMR) and 4-(4'-methylaminophenylazo) benzoic acid (Dabcyl), respectively. In the absence of NC, cTAR is mainly in a non-fluorescent closed form where the TMR and Dabcyl labels are close together, giving excitonic coupling (51). The destabilization was measured through the fluorescence intensity increase of TMR in the labeled cTAR as a function of NC(11-55) concentration (43, 52).

The ability of the labeled peptides to promote the annealing of cTAR (55 base hairpin DNA) with its complementary dTAR sequence was compared to that of the unlabeled NC peptide (53). The kinetic measurements were performed under pseudo-first-order conditions by using unlabeled dTAR at a concentration which was 30-fold higher than the concentration of cTAR labeled with carboxytetramethylrhodamine (TMR) at the 5' end and with 5/6-carboxyfluorescein (Fl) at the 3' end (53). Excitation and emission wavelengths were 480 and 520 nm, respectively, for monitoring the Fl fluorescence. All reported concentrations correspond to those after mixing. To avoid high local concentrations during mixing, both reactants were mixed at the same volume. Peptides were added to each reactant separately at a peptide:ODN ratio of 3:1, and then, the reaction was initiated by mixing the peptide-coated ODNs together. Experiments were performed in 25 mM Tris, 30 mM NaCl, 0.2 mM MgCl<sub>2</sub>, pH 7.5 at 20 °C.

## Results and discussion

To obtain the L-amino acid bearing the 3HC fluorophore, we started with L-tyrosine that was converted into corresponding acetophenone **1** using a described procedure (47, 48) based on Fries reaction (Scheme 1). Then, the amino group was protected with the Boc group, and the product **2** was condensed with furfuraldehyde in the presence of a base. The obtained chalcone **3** was further converted into a 3HC derivative (Boc-3HCaa) using Algar-Flynn-Oyamada reaction. Then, the Boc group was removed to obtain the desired amino acid (3HCaa). Finally, it was protected with the Fmoc group, which is required for solid phase peptide synthesis. We checked that the basic conditions used in the synthesis do not alter the optical purity of the obtained amino acid. For this purpose, the obtained Boc-protected amino acid was first benzylated, then the amino group was deprotected and finally modified with (R)- and (S)-Mosher agents (Scheme S2, Supporting Information). The  $^{19}\text{F}$ -NMR spectra of the two products **9** and **10** showed only one fluorine peak corresponding to pure diastereomers, indicating that the synthesis did not produce any racemization. This conclusion was confirmed by  $^1\text{H}$ -NMR spectra of these two diastereomers.



**Scheme 1.** Synthesis of the fluorescent amino acid and the labelled peptides. The substituted positions of the NC(11-55) peptide are shown by blue arrows.

Then, the spectroscopic properties of the new amino acid (Boc-3HCaa) were characterized in different solvents (Figure 2, Table S1, Supporting Information). The absorption and emission maxima of Boc-3HCaa were remarkably close to those reported previously for the basic fluorophore FHC (Table S1) (24), indicating that 6-substitution in this fluorophore did not change its spectroscopic properties. The dual emission of Boc-3HCaa was found to depend strongly on solvent polarity, showing an increase of

the relative intensity of the N\* band in more polar solvents (Figure 2A) due to an inhibition of the ESPT reaction (8). However, it should be noted that the ratio of the two emission bands of Boc-3HCaa in polar protic solvents is considerably lower than that of the parent fluorophore, indicating that the Boc-protected amino acid group screens partially the fluorophore from polar solvents. Therefore, to estimate the local water concentration, we used the calibration curve  $\log(N^*/T^*)$  vs water concentration previously reported for the parent FHC dye (Figure 2B) (28).

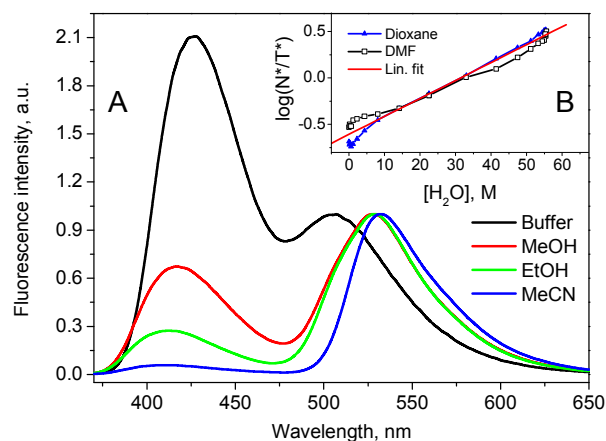


**Figure 2.** Fluorescence spectra of the Boc-3HCaa derivative in different solvents (A) and dependence of  $\log(N^*/T^*)$  of 2-(2-furyl)-3HC (FHC) on water concentration in organic solvents based on data from (28) (B). In (A), 10 mM phosphate buffer, 30 mM NaCl, pH = 6.5 was used. All the spectra were normalized at the T\* band. Excitation wavelength was 350 nm. Concentration of Boc-3HCaa was 1  $\mu$ M.

Using the Fmoc-protected 3HCaa, we then synthesized two labeled NC(11-55) peptides: NC(11-55)-A30-3HCaa and NC(11-55)-W37-3HCaa, where the fluorescent amino acid substituted Ala30 and Trp37 residues, located in the linker and the distal zinc finger, respectively (Scheme 1). Importantly, the 3HCaa was compatible with the standard protocols of peptide synthesis and purification. The NOESY spectra show that the folding of the zinc fingers is maintained in the two labeled NC(11-55) peptides (Figure S2, supporting information), since similar medium and long distance NOEs were found as for the native peptide. Thus, the incorporated amino acid analogue 3HCaa does not significantly affect the native folding in the two labeled peptides.

Next, we compared the chaperone activity of the labeled peptides with that of the native peptide. First, we checked the ability of the peptides to promote destabilization of DNA stem-loops, such as for instance the cTAR sequence involved in the first strand transfer of reverse transcription (40). This test is particularly important, because substitution of Trp37 in NC(11-55) for a non-aromatic amino acid

results in the loss of this component of NC chaperone activity (40). Remarkably, NC(11-55)-W37-3HCaa showed high destabilization activity, nearly identical to that of the native peptide, while NC(11-55)-A30-3HCaa was less active (Figure 3). Secondly, we tested the ability of the labeled peptides to promote the annealing of two complementary sequences. Both labeled peptides exhibited similar activities comparable to that of the native peptide (Figure S3, supporting information), indicating that this component of NC chaperone activity is also preserved. The preserved chaperone activity of NC(11-55)-W37-3HCaa shows that the new amino acid does not affect the peptide folding and can functionally substitute the Trp37 residue. We could explain this outstanding feature of the new amino acid by the two factors. Firstly, similarly to Trp, 3HCaa bears a flat and relatively small aromatic moiety. Secondly, the 3HC moiety, due to its compact structure, can easily intercalate within the nucleobases, as it was shown in different recent reports (26, 27, 54). This property allows 3HC moiety to mimic the interaction of Trp37 indole moiety with nucleobases in the complexes of the peptide with nucleic acid sequences (34-36, 38).

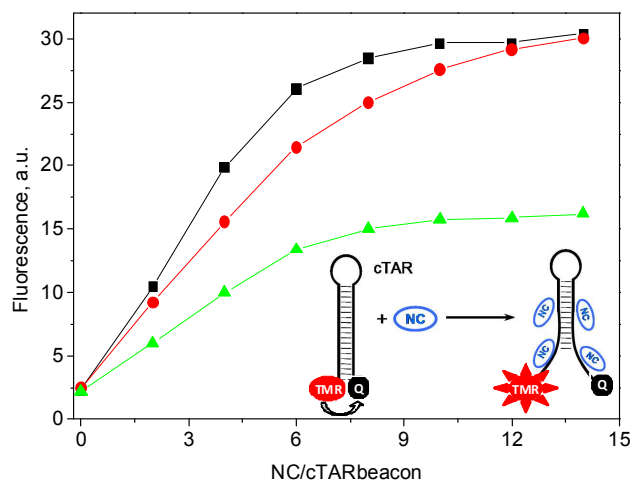


**Figure 3.** Destabilization of doubly-labelled cTAR DNA by NC(11-55) (squares), NC(11-55)-W37-3HCaa (disks) and NC(11-55)-A30-3HCaa (triangles). Titration of 100 nM Dabcyl-5'-cTAR-3'-TMR by NC peptides was performed in 25 mM TRIS (pH 7.5), 30 mM NaCl and 0.2 mM MgCl<sub>2</sub>. To monitor TMR fluorescence, excitation wavelength was set at 520 nm.

**Table 1.** Spectroscopic properties of the 3HCaa-labeled NC(11-55) peptides in complexes with ODNs.<sup>a</sup>

Peptide	Oligo-nucleotide	$\lambda_{\text{ABS}}$ nm	$\lambda_{\text{N}^*}$ nm	$\lambda_{\text{T}^*}$ nm	$\text{N}^*/\text{T}^*$	$[\text{H}_2\text{O}]$ , M	$W_{\text{A}}$	QY, %
	-	364	426	520	0.57	31	0.56	3.7
NC(11-55)- A30-3HCaa	$\Delta\text{P}(-)$ PBS	364	425	526	0.46	27	0.49	2.5
	SL3	363	426	523	0.57	30	0.54	2.5
	SL2	363	426	523	0.54	30	0.54	2.5
	-	366	427	522	0.61	32	0.58	9.0
NC(11-55)- W37-3HCaa	$\Delta\text{P}(-)$ PBS	367	425	534	0.33	23	0.41	5.1
	SL3	368	427	531	0.29	21	0.38	4.0
	SL2	368	425	533	0.24	18	0.32	4.8

<sup>a</sup>  $\lambda_{\text{ABS}}$ ,  $\lambda_{\text{N}^*}$  and  $\lambda_{\text{T}^*}$  are the maxima of absorption,  $\text{N}^*$  and  $\text{T}^*$  emission bands, respectively;  $\text{N}^*/\text{T}^*$  is the intensity ratio of the two emission bands measured at the peak maxima (error  $\pm 5\%$ );  $[\text{H}_2\text{O}]$  is the water concentration estimated using a method reported elsewhere (error  $\pm 1\text{M}$ );  $W_{\text{A}}$  is water access coefficient (28); QY is the fluorescence quantum yield. Excitation wavelength was 350 nm. Measurements were done in 10 mM phosphate buffer, 30 mM NaCl, pH 6.5. Peptide and ODN concentrations were 1  $\mu\text{M}$ .

Labeled peptides in aqueous solutions (Figure 4) showed dual emission, characteristic of 3HC dyes, where the short- and long-wavelength bands can be assigned to  $\text{N}^*$  and  $\text{T}^*$  forms, respectively. The observed intensity ratio of the two emission bands,  $\text{N}^*/\text{T}^*$ , is close to that for the FHC fluorophore in ethanol (Tables 1 and S1, Supporting Information), indicating that the 3HCaa fluorophore is partially screened from water by the peptide in its folded form. Using a recently developed method (28), the local water concentration  $[\text{H}_2\text{O}]_{\text{L}}$  of the 3HCaa solvation shell in both peptides was estimated around 31-32 M (Table 1), which corresponds to a water access coefficient  $W_{\text{A}}$  for the probe of 0.57 ( $W_{\text{A}} = [\text{H}_2\text{O}]_{\text{L}} / [\text{H}_2\text{O}]$ , where  $[\text{H}_2\text{O}] = 55.56\text{ M}$  is the concentration of neat water). This estimation indicates that almost half of the space around the 3HC fluorophore is screened from the bulk water by the peptide backbone.

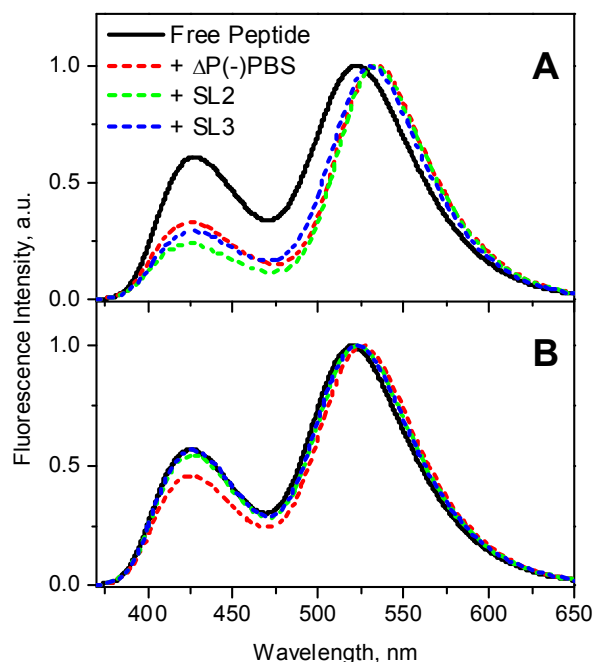


**Figure 4.** Effect of ODN interaction on the fluorescence spectra of the 3HCaa-labeled NC(11-55) peptides. Fluorescence spectra of NC(11-55)-W37-3HCaa (A) and NC(11-55)-A30-3HCaa (B) were normalized at the T\* band. Peptide and ODN concentrations were 1  $\mu$ M. Measurements were done in 10 mM phosphate buffer, 30 mM NaCl, pH 6.5. Excitation wavelength was 350 nm.

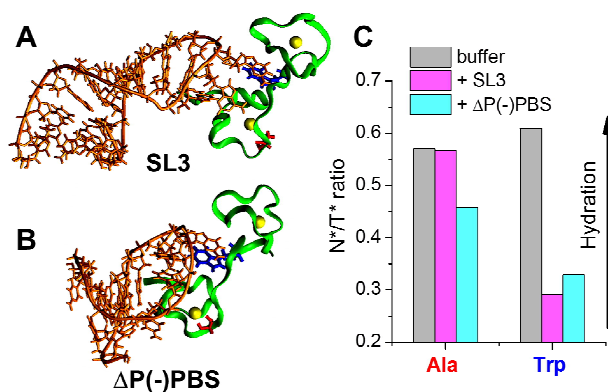


**Figure 5.** Correlation between the 3D structures of NC-ODN complexes and the response of the 3HCaa-labeled peptides on ODN binding. 3D structures of NC complexes with SL3 (A) and  $\Delta P(-)PBS$  (B) drawn based on NMR data (34, 36). Only the NC(11-55) part is shown on the figures. Zn atoms are represented as yellow spheres, Ala30 and Trp37 residues are in red, and blue, respectively. Fluorescence intensity ratio N\*/T\* for NC(11-55)-A30-3HCaa (Ala) and NC(11-55)-W37-3HCaa (Trp) peptides in buffer and bound to SL3 or  $\Delta P(-)PBS$  (C).

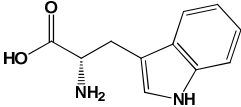
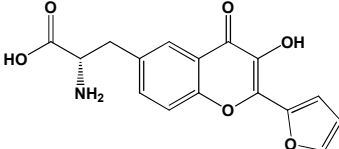
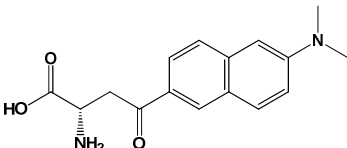
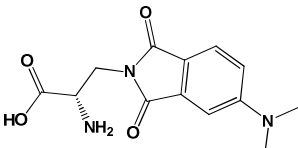
On interaction with ODNs SL2, SL3 and  $\Delta P(-)$ PBS, a strong change in the NC(11-55)-W37-3HCaa fluorescence spectrum was observed, with notably a large drop in the  $N^*/T^*$  ratio, a shift of the  $T^*$  emission maximum to the red (Figure 5) and a decrease in the fluorescence quantum yield (Table 1). The drop in the  $N^*/T^*$  ratio can be assigned to a decrease in the local hydration of the 3HCaa environment, with a water access coefficient  $W_A$  of the probe dropping to 0.32-0.41 for the three ODNs (Table 1). The observed dehydration is likely connected to the interaction of the 3HC fluorophore with the nucleobases, which leads to an efficient screening of this fluorophore from water (26, 27). Moreover, this conclusion is substantiated by the observed red shift of the  $T^*$  band (26, 27) and is in line with the NMR-derived 3D structures of the NC-ODN complexes (Figure 5), showing that the Trp37 residue strongly interacts with the nucleobases (34-36, 38). Therefore, this observation further confirms that the 3HCaa can mimic the Trp residue at position 37. In contrast, binding of NC(11-55)-A30-3HCaa to the three ODNs led to either no change (with SL2 and SL3) or a limited decrease (with  $\Delta P(-)$ PBS) in the  $N^*/T^*$  ratio with a slight decrease in its quantum yield (Table 1) and almost negligible spectral shifts of the absorption and emission maxima (Table 1). The absence of changes in the  $N^*/T^*$  ratio observed with the SL2 and SL3 sequences can be rationalized by the large distance between the A30 residue and the nucleobases in the NC-ODN complexes (Figure 5). As a consequence, the 3HCaa at position 30 in the complexes with SL2 and SL3 cannot interact with the ODN and remains highly exposed to water, as in the free peptide. Finally, the moderate change in the  $N^*/T^*$  ratio observed when NC(11-55)-A30-3HCaa was complexed with  $\Delta P(-)$ PBS is fully consistent with the closer proximity of the Ala30 residue to the  $\Delta P(-)$ PBS nucleobases, as compared to that in the complexes with SL2 and SL3 (34, 36, 38).

Finally, using the changes in the  $N^*/T^*$  ratio or the quantum yield of 3HCaa as an analytical signal of interaction, we further measured the binding constant of the three labeled peptides to SL3. The obtained binding constants matched closely that obtained with the native peptide (Table S2, Supporting Information) (35, 37), indicating that the incorporated 3HCaa probe did not change the binding affinity of the peptides and could thus be also used for quantification of peptide-ODN interaction. Since Trp37 was shown to be critical for the high affinity of NC to its target ODNs (40, 42, 45), this indicates that the substitution of Trp37 by 3HCaa does not alter the ability of NC to recognize its ODN targets. The results are in line with the peptide activity tests and NMR structural data, providing a clear background for considering 3HCaa as new amino acid analogue that can readily substitute Trp even at the places where it plays a crucial role in the peptide.

Though the  $N^*/T^*$  ratio of 3HCaa is mostly controlled by the environment polarity and hydration, we could not exclude possible quenching effects, which are frequently observed for dyes interacting with

nucleobases (35, 41). Indeed, the  $N^*/T^*$  ratio could decrease for instance due to a more efficient quenching of the  $N^*$  state compared to the  $T^*$  state, as a consequence of static or dynamic quenching by the neighbor nucleobases. However, we expect this effect to be minor in the probe response because the red shift of the  $T^*$  band produced by peptide-DNA interaction correlates well with the changes in the  $N^*/T^*$  ratio (Table 1). As this red shift is directly linked to the dehydration of the dye environment (26, 27, 55) and not to quenching, the ratio changes appear mainly driven by the dehydration within the peptide-DNA complex. Moreover, as the  $N^*$  and  $T^*$  states are coupled by the ESIPT reaction, the quenching of the  $N^*$  state should influence the  $N^*/T^*$  ratio to a less significant extent, compared to the case where the two states are independent.

**Table 2.** Spectroscopic properties and response to environment of the new 3HC amino acid in comparison to other amino acid analogues.<sup>a</sup>

Amino acid	Fluoro- phore	$\lambda_{\text{abs}}$ (nm) EtOH	$\varepsilon$ (M <sup>-1</sup> cm <sup>-1</sup> )	$\lambda_{\text{em}}$ (nm) EtOH	$\lambda_{\text{em}}$ (nm) Water	$\Delta\lambda$ (nm)	Refs
	Indole	280	5500	342	355	13	(56)
	FHC	360	16000	531	427	-104	-
	Prodan	360	18400	496	531	35	(5, 9, 57)
	4- DMAP	408	6500	534 <sup>b</sup>	562	28	(11, 58)

<sup>a</sup>  $\lambda_{\text{abs}}$  and  $\lambda_{\text{em}}$  – absorption and emission maxima of the fluorophores in the corresponding solvent;  $\varepsilon$  – absorption coefficient of the fluorophore in ethanol;  $\Delta\lambda$  – shift of the emission maximum in response to changes in the solvent polarity (water vs ethanol); <sup>b</sup> data in methanol.

Compared to Trp, the new fluorophore features strongly red shifted absorption and emission (Table 2), allowing more convenient spectroscopic studies in biological samples with less background noise and photo-damage. Moreover, it preserves its fluorescence on peptide binding to nucleic acids, while Trp is frequently quenched (35, 41). Moreover, due to ESIPT, it presents much higher sensitivity to the

environment in high-polarity range, so that it almost switches its fluorescence from dominant T\* emission in ethanol (at 531 nm) to dominant N\* emission in water (at 427 nm), while Trp in these conditions changes its emission maximum only by a few nm (56). This exclusive environment sensitivity places it in front of all other existing fluorescent amino acid analogues of similar small size, based on Prodan and 4-DMAP (Table 2). Indeed, for highly polar environments (alcohols and water), the fluorophore of the new amino acid (FHC) is about 3-fold more sensitive to solvent polarity (hydration) as compared to Prodan and 4-DMAP. Moreover, the FHC provides an opportunity to quantitatively evaluate the hydration in the site of interaction between the two biomolecules. These exclusive properties originate from the strong effect of H-bonding solvents on the ESIPT reaction in these derivatives (15). As peptides and nucleic acids present rather highly polar micro-environments, the new amino acid constitutes a unique tool for probing interactions of these biomolecules in a site specific manner.

## Conclusion

For the first time, a fluorescent L-amino acid, exhibiting ESIPT and hydration-sensitive dual emission, was synthesized. This amino acid bears as a side chain, the 2-(2-furyl)-3-hydroxychromone fluorophore, which is flat and close in size to the indole moiety of L-Tryptophan. It was incorporated at two different positions of the NC(11-55) peptide. Remarkably, substitution of the highly conserved Trp37 residue by this fluorescent amino acid was found to preserve both the native folding and chaperone activity of the peptide. Interaction of the labeled peptides with target ODNs changed dramatically the dual emission of the incorporated amino acid and these changes depended on its position in the peptide and on the ODN sequence. The obtained results established a correlation between the fluorescence response of the amino acid probe and its proximity to the interacting ODN bases. This amino acid appears as an attractive tool for probing the binding sites in peptide-nucleic acid complexes, being particularly suitable to substitute tryptophan residues. Compared to tryptophan and its close fluorescent analogues, this new amino acid presents superior environment sensitivity.

## Acknowledgment

This work, VYP and VGP were supported by ANR (ANR-07-BLAN-0287), ANR Femtostack, ANRS, CNRS and Université de Strasbourg. OVS was supported by ARCUS Alsace. We thank to Cyril Antheaume and Patrick Wehrung for NMR and Mass measurements, respectively.

**Supporting Information Available:** Additional characterization data on the fluorescent amino acid and its peptide conjugates and the studied ODN sequences are presented. This material is available free of charge via the Internet at <http://pubs.acs.org>.

## References

1. Mikhailiuk, P. K., Afonin, S., Chernega, A. N., Rusanov, E. B., Platonov, M. O., Dubinina, G. G., Berditsch, M., Uirich, A. S., and Komarov, I. V. (2006) Conformationally rigid trifluoromethyl-substituted alpha-amino acid designed for peptide structure analysis by solid-state F-19 NMR spectroscopy, *Angew. Chem.-Int. Edit.* **45**, 5659-5661.
2. Mizukami, S., Takikawa, R., Sugihara, F., Shirakawa, M., and Kikuchi, K. (2009) Dual-Function Probe to Detect Protease Activity for Fluorescence Measurement and F-19 MRI, *Angew. Chem.-Int. Ed.* **48**, 3641-3643.
3. Ieronimo, M., Afonin, S., Koch, K., Berditsch, M., Wadhwani, P., and Ulrich, A. S. (2010) F-19 NMR Analysis of the Antimicrobial Peptide PGLa Bound to Native Cell Membranes from Bacterial Protoplasts and Human Erythrocytes, *J. Am. Chem. Soc.* **132**, 8822-+.
4. de Villiers, J., Koekemoer, L., and Strauss, E. (2010) 3-Fluoroaspartate and Pyruvoyl-Dependant Aspartate Decarboxylase: Exploiting the Unique Characteristics of Fluorine To Probe Reactivity and Binding, *Chem.-Eur. J.* **16**, 10030-10041.
5. Cohen, B. E., McAnaney, T. B., Park, E. S., Jan, Y. N., Boxer, S. G., and Jan, L. Y. (2002) Probing protein electrostatics with a synthetic fluorescent amino acid, *Science* **296**, 1700-1703.
6. Brun, M. P., Bischoff, L., and Garbay, C. (2004) A very short route to enantiomerically pure coumarin-bearing fluorescent amino acids, *Angew. Chem.-Int. Ed.* **43**, 3432-3436.
7. Venkatraman, P., Nguyen, T. T., Sainlos, M., Bilsel, O., Chitta, S., Imperiali, B., and Stern, L. J. (2007) Fluorogenic probes for monitoring peptide binding to class II MHC proteins in living cells, *Nat. Chem. Biol.* **3**, 222-228.
8. Demchenko, A. P., Mely, Y., Duportail, G., and Klymchenko, A. S. (2009) Monitoring biophysical properties of lipid membranes by environment-sensitive fluorescent probes, *Biophys. J.* **96**, 3461-3470.
9. Nitz, M., Mezo, A. R., Ali, M. H., and Imperiali, B. (2002) Enantioselective synthesis and application of the highly fluorescent and environment-sensitive amino acid 6-(2-dimethylaminonaphthoyl) alanine (DANA), *Chem Commun (Camb)*, 1912-1913.
10. Chen, H., Chung, N. N., Lemieux, C., Zelent, B., Vanderkooi, J. M., Gryczynski, I., Wilkes, B. C., and Schiller, P. W. (2005) [Aladan3]TIPP: a fluorescent delta-opioid antagonist with high delta-receptor binding affinity and delta selectivity, *Biopolymers* **80**, 325-331.
11. Vazquez, M. E., Rothman, D. M., and Imperiali, B. (2004) A new environment-sensitive fluorescent amino acid for Fmoc-based solid phase peptide synthesis, *Org. Biomol. Chem.* **2**, 1965-1966.
12. Vazquez, M. E., Blanco, J. B., and Imperiali, B. (2005) Photophysics and biological applications of the environment-sensitive fluorophore 6-N,N-dimethylamino-2,3-naphthalimide, *J Am Chem Soc* **127**, 1300-1306.
13. Loving, G., and Imperiali, B. (2008) A versatile amino acid analogue of the solvatochromic fluorophore 4-N,N-dimethylamino-1,8-naphthalimide: a powerful tool for the study of dynamic protein interactions, *J Am Chem Soc* **130**, 13630-13638.
14. Sengupta, P. K., and Kasha, M. (1979) Excited state proton-transfer spectroscopy of 3-hydroxyflavone and quercetin, *Chem. Phys. Lett.* **68**, 382-385.

15. Das, R., Klymchenko, A. S., Duportail, G., and Mely, Y. (2009) Unusually slow proton transfer dynamics of a 3-hydroxychromone dye in protic solvents, *Photochem. Photobiol. Sci.* **8**, 1583-1589.
16. Shynkar, V. V., Klymchenko, A. S., Piemont, E., Demchenko, A. P., and Mely, Y. (2004) Dynamics of intermolecular hydrogen bonds in the excited states of 4'-dialkylamino-3-hydroxyflavones. On the pathway to an ideal fluorescent hydrogen bonding sensor, *J. Phys. Chem. A* **108**, 8151-8159.
17. Enander, K., Choulier, L., Olsson, A. L., Yushchenko, D. A., Kanmert, D., Klymchenko, A. S., Demchenko, A. P., Mely, Y., and Altschuh, D. (2008) A peptide-based, ratiometric biosensor construct for direct fluorescence detection of a protein analyte, *Bioconjugate Chem.* **19**, 1864-1870.
18. Chou, P.-T., Martinez, M. L., and Clements, H. (1993) Reversal of excitation behavior of proton-transfer vs. charge-transfer by dielectric perturbation of electronic manifolds, *J. Phys. Chem.* **97**, 2618-2622.
19. Ormson, S. M., Brown, R. G., Vollmer, F., and Rettig, W. (1994) Switching between charge- and proton-transfer emission in the excited state of a substituted 3-hydroxyflavone, *J. Photochem. Photobiol., A* **81**, 65-72.
20. Swinney, T. C., and Kelley, D. F. (1993) Proton transfer dynamics in substituted 3-hydroxyflavones: Solvent polarization effects, *J. Chem. Phys.* **99**, 211-221.
21. Klymchenko, A. S., and Demchenko, A. P. (2003) Multiparametric probing of intermolecular interactions with fluorescent dye exhibiting excited state intramolecular proton transfer, *Phys. Chem. Chem. Phys.* **5**, 461-468.
22. Strandjord, A. J. G., and Barbara, P. F. (1985) Proton-transfer kinetics of 3-hydroxyflavone: Solvent effects, *J. Phys. Chem.* **89**, 2355.
23. McMorro, D., and Kasha, M. (1984) Intramolecular excited-state proton transfer in 3-hydroxyflavone. Hydrogen-bonding solvent perturbations, *J. Phys. Chem.* **88**, 2235-2243.
24. Klymchenko, A. S., and Demchenko, A. P. (2004) 3-Hydroxychromone dyes exhibiting excited-state intramolecular proton transfer in water with efficient two-band fluorescence, *New J. Chem.* **28**, 687.
25. Yushchenko, D. A., Fauerbach, J. A., Thirunavukkuarasu, S., Jares-Erijman, E. A., and Jovin, T. M. (2010) Fluorescent Ratiometric MFC Probe Sensitive to Early Stages of alpha-Synuclein Aggregation, *J. Am. Chem. Soc.* **132**, 7860-7861.
26. Klymchenko, A. S., Shvadchak, V. V., Yushchenko, D. A., Jain, N., and Mely, Y. (2008) Excited-state intramolecular proton transfer distinguishes microenvironments in single-and double-stranded DNA, *J. Phys. Chem. B* **112**, 12050.
27. Shvadchak, V. V., Klymchenko, A. S., De Rocquigny, H., and Mely, Y. (2009) Sensing peptide - Oligonucleotide interactions by a two-color fluorescence label: Application to the HIV-1 nucleocapsid protein, *Nucleic Acids Res.* **37**, e25.
28. Pivovarenko, V. G., Zamotaiev, O. M., Shvadchak, V. V., Postupalenko, V. Y., Klymchenko, A. S., and Mély, Y. (2012) Quantification of local hydration at the surface of biomolecules using dual-fluorescence labels, *J. Phys. Chem. A* **116**, 3103-3109.
29. Thomas, J. A., and Gorelick, R. J. (2008) Nucleocapsid protein function in early infection processes, *Virus Res.* **134**, 39-63.
30. Darlix, J. L., Godet, J., Ivanyi-Nagy, R., Fosse, P., Mauffret, O., and Mely, Y. (2011) Flexible nature and specific functions of the HIV-1 Nucleocapsid protein, *J. Mol. Biol.* **410**, 565-581.
31. Summers, M. F., Henderson, L. E., Chance, M. R., Bess Jr, J. W., South, T. L., Blake, P. R., Sagi, I., Perez-Alvarado, G., Sowder III, R. C., Hare, D. R., and Arthur, L. O. (1992) Nucleocapsid zinc fingers detected in retroviruses: EXAFS studies of intact viruses and the solution-state structure of the nucleocapsid protein from HIV-1, *Protein Sci.* **1**, 563-574.

- 1  
2  
3  
4  
5  
6  
7  
8  
9  
10  
11  
12  
13  
14  
15  
16  
17  
18  
19  
20  
21  
22  
23  
24  
25  
26  
27  
28  
29  
30  
31  
32  
33  
34  
35  
36  
37  
38  
39  
40  
41  
42  
43  
44  
45  
46  
47  
48  
49  
50  
51  
52  
53  
54  
55  
56  
57  
58  
59  
60
32. Morellet, N., Jullian, N., De Rocquigny, H., Maigret, B., Darlix, J. L., and Roques, B. P. (1992) Determination of the structure of the nucleocapsid protein NCp7 from the human immunodeficiency virus type 1 by <sup>1</sup>H NMR, *EMBO J.* **11**, 3059-3065.
33. Clever, J., Sasseti, C., and Parslow, T. G. (1995) RNA secondary structure and binding sites for gag gene products in the 5' packaging signal of human immunodeficiency virus type 1, *J. Virol.* **69**, 2101-2109.
34. de Guzman, R. N., Wu, Z. R., Stalling, C. C., Pappalardo, L., Borer, P. N., and Summers, M. F. (1998) Structure of the HIV-1 nucleocapsid protein bound to the SL3  $\Psi$ -RNA recognition element, *Science* **279**, 384-388.
35. Vuilleumier, C., Bombarda, E., Morellet, N., Gerard, D., Roques, B. P., and Mely, Y. (1999) Nucleic acid sequence discrimination by the HIV-1 nucleocapsid protein NCp7: a fluorescence study, *Biochemistry* **38**, 16816-16825.
36. Bourbigot, S., Ramalanjaona, N., Boudier, C., Salgado, G. F. J., Roques, B. P., Mely, Y., Bouaziz, S., and Morellet, N. (2008) How the HIV-1 Nucleocapsid Protein Binds and Destabilises the (-)Primer Binding Site During Reverse Transcription, *J. Mol. Biol.* **383**, 1112-1128.
37. Shubsda, M. F., Paoletti, A. C., Hudson, B. S., and Borer, P. N. (2002) Affinities of packaging domain loops in HIV-1 RNA for the nucleocapsid protein, *Biochemistry* **41**, 5276-5282.
38. Amarasinghe, G. K., De Guzman, R. N., Turner, R. B., Chancellor, K. J., Wu, Z. R., and Summers, M. F. (2000) NMR structure of the HIV-1 nucleocapsid protein bound to stem-loop SL2 of the Psi-RNA packaging signal. Implications for genome recognition, *J. Mol. Biol.* **301**, 491-511.
39. Fisher, R. J., Rein, A., Fivash, M., Urbaneja, M. A., Casas-Finet, J. R., Medaglia, M., and Henderson, L. E. (1998) Sequence-specific binding of human immunodeficiency virus type 1 nucleocapsid protein to short oligonucleotides, *J. Virol.* **72**, 1902-1909.
40. Beltz, H., Clauss, C., Piemont, E., Ficheux, D., Gorelick, R. J., Roques, B., Gabus, C., Darlix, J. L., de Rocquigny, H., and Mely, Y. (2005) Structural determinants of HIV-1 nucleocapsid protein for cTAR DNA binding and destabilization, and correlation with inhibition of self-primed DNA synthesis, *J. Mol. Biol.* **348**, 1113-1126.
41. Mely, Y., de Rocquigny, H., Sorinasjimeno, M., Keith, G., Roques, B. P., Marquet, R., and Gerard, D. (1995) Binding Of The HIV-1 Nucleocapsid Protein To The Primer tRNA(3)(Lys), In-Vitro, Is Essentially Not Specific, *J. Biol. Chem.* **270**, 1650-1656.
42. Godet, J., Ramalanjaona, N., Sharma, K. K., Richert, L., De Rocquigny, H., Darlix, J. L., Duportail, G., and Mély, Y. (2011) Specific implications of the HIV-1 nucleocapsid zinc fingers in the annealing of the primer binding site complementary sequences during the obligatory plus strand transfer, *Nucleic Acids Res.* **39**, 6633-6645.
43. Bernacchi, S., Stoylov, S., Piemont, E., Ficheux, D., Roques, B. P., Darlix, J. L., and Mely, Y. (2002) HIV-1 nucleocapsid protein activates transient melting of least stable parts of the secondary structure of TAR and its complementary sequence, *J. Mol. Biol.* **317**, 385-399.
44. Post, K., Kankia, B., Gopalakrishnan, S., Yang, V., Cramer, E., Saladores, P., Gorelick, R. J., Guo, J. H., Musier-Forsyth, K., and Levin, J. G. (2009) Fidelity of plus-strand priming requires the nucleic acid chaperone activity of HIV-1 nucleocapsid protein, *Nucleic Acids Res.* **37**, 1755-1766.
45. Avilov, S. V., Piemont, E., Shvadchak, V., de Rocquigny, H., and Mely, Y. (2008) Probing dynamics of HIV-1 nucleocapsid protein/target hexanucleotide complexes by 2-aminopurine, *Nucleic Acids Res.* **36**, 885-896.
46. Dorfman, T., Luban, J., Goff, S. P., Haseltine, W. A., and Gottlinger, H. G. (1993) Mapping of functionally important residues of a cysteine-histidine box in the human immunodeficiency virus type 1 nucleocapsid protein, *J. Virol.* **67**, 6159-6169.

47. Hufford, C. D., Oguntimein, B. O., and Shoolery, J. N. (1987) Angoluarin, an antimicrobial dihydrochalcone from *Uvaria angolensis*, *J. Org. Chem.* **52**, 5286-5288.
48. Chen, C., Zhu, Y. F., and Wilcoxon, K. (2000) An improved synthesis of selectively protected L-Dopa derivatives from L-tyrosine, *J. Org. Chem.* **65**, 2574-2576.
49. De Rocquigny, H., Ficheux, D., Gabus, C., Fournie-Zaluski, M. C., Darlix, J. L., and Roques, B. P. (1991) First large scale chemical synthesis of the 72 amino acid HIV-1 nucleocapsid protein NCp7 in an active form, *Biochem. Biophys. Res. Comm.* **180**, 1010-1018.
50. Eastman, J. W. (1967) *Photochem. Photobiol.* **6**, 55.
51. Bernacchi, S., Piémont, E., Potier, N., Van Dorsselaer, A., and Mély, Y. (2003) Excitonic heterodimer formation in an HIV-1 oligonucleotide labeled with a donor-acceptor pair used for fluorescence resonance energy transfer, *Biophys. J.* **84**, 643-654.
52. Beltz, H., Azoulay, J., Bernacchi, S., Clamme, J. P., Ficheux, D., Roques, B., Darlix, J. L., and Mely, Y. (2003) Impact of the terminal bulges of HIV-1 cTAR DNA on its stability and the destabilizing activity of the nucleocapsid protein NCp7, *J. Mol. Biol.* **328**, 95-108.
53. Godet, J., de Rocquigny, H., Raja, C., Glasser, N., Ficheux, D., Darlix, J. L., and Mely, Y. (2006) During the early phase of HIV-1 DNA synthesis, nucleocapsid protein directs hybridization of the TAR complementary sequences via the ends of their double-stranded stem, *J. Mol. Biol.* **356**, 1180-1192.
54. Dziuba, D., Postupalenko, V. Y., Spadafora, M., Klymchenko, A. S., Guérineau, V., Mély, Y., Benhida, R., and Burger, A. (2012) A universal nucleoside with strong two-band switchable fluorescence and sensitivity to environment for investigating DNA interactions, *J. Am. Chem. Soc.* **134**, 10209-10213.
55. Kenfack, C. A., Klymchenko, A. S., Duportail, G., Burger, A., and Mély, Y. (2012) Ab initio study of the solvent H-bonding effect on ESIPT reaction and electronic transitions of 3-hydroxychromone derivatives, *Phys. Chem. Chem. Phys.* **14**, 8910-8918.
56. Lakowicz, J. R. (2006) *Principles of Fluorescence Spectroscopy*, Kluwer Academic, New York.
57. Weber, G., and Farris, F. J. (1979) Synthesis and spectral properties of a hydrophobic fluorescent probe: 6-propionyl-2-(dimethylamino)naphthalene, *Biochemistry* **18**, 3075-3078.
58. Soujanya, T., Fessenden, R. W., and Samanta, A. (1996) Role of nonfluorescent twisted intramolecular charge transfer state on the photophysical behavior of aminophthalimide dyes, *J. Phys. Chem.* **100**, 3507.

### Table of Contents artwork:

